Observation of an Anomalous Line Shape of the $\eta'\pi^+\pi^-$ Mass Spectrum near the $p\bar{p}$ Mass Threshold in $J/\psi \to \gamma\eta'\pi^+\pi^-$

M. Ablikim,[1] M. N. Achasov,[9,e] S. Ahmed,[14] X. C. Ai,[1] O. Albayrak,[5] M. Albrecht,[4] D. J. Ambrose,[44] A. Amoroso,[49a,49c] F. F. An,[1] Q. An,[46,a] J. Z. Bai,[1] R. Baldini Ferroli,[20a] Y. Ban,[31] D. W. Bennett,[19] J. V. Bennett,[5] N. Berger,[22] M. Bertani,[20a] D. Bettoni,[21a] J. M. Bian,[43] F. Bianchi,[49a,49c] E. Boger,[23,c] I. Boyko,[23] R. A. Briere,[5] H. Cai,[51] X. Cai,[1,a] O. Cakir,[40a] A. Calcaterra,[20a] G. F. Cao,[1] S. A. Cetin,[40b] J. F. Chang,[1,a] G. Chelkov,[23,c,d] G. Chen,[1] H. S. Chen,[1] H. Y. Chen,[2] J. C. Chen,[1] M. L. Chen,[1,a] S. Chen,[41] S. J. Chen,[29] X. Chen,[1,a] X. R. Chen,[26] Y. B. Chen,[1,a] H. P. Cheng,[17] X. K. Chu,[31] G. Cibinetto,[21a] H. L. Dai,[1,a] J. P. Dai,[34] A. Dbeyssi,[14] D. Dedovich,[23] Z. Y. Deng,[1] A. Denig,[22] I. Denysenko,[23] M. Destefanis,[49a,49c] F. De Mori,[49a,49c] Y. Ding,[27] C. Dong,[30] J. Dong,[1,a] L. Y. Dong,[1] M. Y. Dong,[1,a] Z. L. Dou,[29] S. X. Du,[53] P. F. Duan,[1] J. Z. Fan,[39] J. Fang,[1,a] S. S. Fang,[1] X. Fang,[46,a] Y. Fang,[1] R. Farinelli,[21a,21b] L. Fava,[49b,49c] O. Fedorov,[23] F. Feldbauer,[22] G. Felici,[20a] C. Q. Feng,[46,a] E. Fioravanti,[21a] M. Fritsch,[14,22] C. D. Fu,[1] Q. Gao,[1] X. L. Gao,[46,a] X. Y. Gao,[2] Y. Gao,[39] Z. Gao,[46,a] I. Garzia,[21a] K. Goetzen,[10] L. Gong,[30] W. X. Gong,[1,a] W. Gradl,[22] M. Greco,[49a,49c] M. H. Gu,[1,a] Y. T. Gu,[12] Y. H. Guan,[1] A. Q. Guo,[1] L. B. Guo,[28] R. P. Guo,[1] Y. Guo,[1] Y. P. Guo,[22] Z. Haddadi,[25] A. Hafner,[22] S. Han,[51] X. Q. Hao,[15] F. A. Harris,[42] K. L. He,[1] F. H. Heinsius,[4] T. Held,[4] Y. K. Heng,[1,a] T. Holtmann,[4] Z. L. Hou,[1] C. Hu,[28] H. M. Hu,[1] J. F. Hu,[49a,49c] T. Hu,[1,a] Y. Hu,[1] G. S. Huang,[46,a] Y. P. Huang,[1,i] J. S. Huang,[15] X. T. Huang,[33] X. Z. Huang,[29] Y. Huang,[29] Z. L. Huang,[27] T. Hussain,[48] Q. Ji,[1] Q. P. Ji,[30] X. B. Ji,[1] X. L. Ji,[1,a] L. W. Jiang,[51] X. S. Jiang,[1,a] X. Y. Jiang,[30] J. B. Jiao,[33] Z. Jiao,[17] D. P. Jin,[1,a] S. Jin,[1] T. Johansson,[50] A. Julin,[43] N. Kalantar-Nayestanaki,[25] X. L. Kang,[1] X. S. Kang,[30] M. Kavatsyuk,[25] B. C. Ke,[5] P. Kiese,[22] R. Kliemt,[14] B. Kloss,[22] O. B. Kolcu,[40b,h] B. Kopf,[4] M. Kornicer,[42] A. Kupsc,[50] W. Kühn,[24] J. S. Lange,[24] M. Lara,[19] P. Larin,[14] H. Leithoff,[22] C. Leng,[49c] C. Li,[50] Cheng Li,[46,a] D. M. Li,[53] F. Li,[1,a] F. Y. Li,[31] G. Li,[1] H. B. Li,[1] H. J. Li,[1] J. C. Li,[1] Jin Li,[32] K. Li,[13] K. Li,[33] Lei Li,[3] P. R. Li,[41] Q. Y. Li,[33] T. Li,[33] W. D. Li,[1] W. G. Li,[1] X. L. Li,[33] X. N. Li,[1,a] X. Q. Li,[30] Y. B. Li,[2] Z. B. Li,[38] H. Liang,[46,a] Y. F. Liang,[36] Y. T. Liang,[24] G. R. Liao,[11] D. X. Lin,[14] B. Liu,[34] B. J. Liu,[1] C. X. Liu,[1] D. Liu,[46,a] F. H. Liu,[35] Fang Liu,[1] Feng Liu,[6] H. B. Liu,[12] H. H. Liu,[1] H. H. Liu,[16] H. M. Liu,[1] J. Liu,[1] J. B. Liu,[46,a] J. P. Liu,[51] J. Y. Liu,[1] K. Liu,[39] K. Y. Liu,[27] L. D. Liu,[31] P. L. Liu,[1,a] Q. Liu,[41] S. B. Liu,[46,a] X. Liu,[26] Y. B. Liu,[30] Y. Y. Liu,[30] Z. A. Liu,[1,a] Zhiqing Liu,[22] H. Loehner,[25] X. C. Lou,[1,a,g] H. J. Lu,[17] J. G. Lu,[1,a] Y. Lu,[1] Y. P. Lu,[1,a] C. L. Luo,[28] M. X. Luo,[52] T. Luo,[42] X. L. Luo,[1,a] X. R. Lyu,[41] F. C. Ma,[27] H. L. Ma,[1] L. L. Ma,[33] M. M. Ma,[1] Q. M. Ma,[1] T. Ma,[1] X. N. Ma,[30] X. Y. Ma,[1,a] Y. M. Ma,[33] F. E. Maas,[14] M. Maggiora,[49a,49c] Q. A. Malik,[48] Y. J. Mao,[31] Z. P. Mao,[1] S. Marcello,[49a,49c] J. G. Messchendorp,[25] G. Mezzadri,[21b] J. Min,[1,a] T. J. Min,[1,41] R. E. Mitchell,[19] X. H. Mo,[1,a] Y. J. Mo,[6] C. Morales Morales,[14] N. Yu. Muchnoi,[9,e] H. Muramatsu,[43] P. Musiol,[4] Y. Nefedov,[23] F. Nerling,[14] I. B. Nikolaev,[9,e] Z. Ning,[1,a] S. Nisar,[8] S. L. Niu,[1,a] X. Y. Niu,[1] S. L. Olsen,[32] Q. Ouyang,[1,a] S. Pacetti,[20b] Y. Pan,[46,a] P. Patteri,[20a] M. Pelizaeus,[4] H. P. Peng,[46,a] K. Peters,[10] J. Pettersson,[50] J. L. Ping,[28] R. G. Ping,[1] R. Poling,[43] V. Prasad,[1] H. R. Qi,[2] M. Qi,[29] S. Qian,[1,a] C. F. Qiao,[41] L. Q. Qin,[33] N. Qin,[51] X. S. Qin,[1] Z. H. Qin,[1,a] J. F. Qiu,[1] K. H. Rashid,[48] C. F. Redmer,[22] M. Ripka,[22] G. Rong,[1] Ch. Rosner,[14] X. D. Ruan,[12] A. Sarantsev,[23,f] M. Savrié,[21b] C. Schnier,[4] K. Schoenning,[50] S. Schumann,[22] W. Shan,[31] M. Shao,[46,a] C. P. Shen,[2] P. X. Shen,[30] X. Y. Shen,[1] H. Y. Sheng,[1] M. Shi,[1] W. M. Song,[1] X. Y. Song,[1] S. Sosio,[49a,49c] S. Spataro,[49a,49c] G. X. Sun,[1] J. F. Sun,[15] S. S. Sun,[1] X. H. Sun,[1] Y. J. Sun,[46,a] Y. Z. Sun,[1] Z. J. Sun,[1,a] Z. T. Sun,[19] C. J. Tang,[36] X. Tang,[1] I. Tapan,[40c] E. H. Thorndike,[44] M. Tiemens,[25] I. Uman,[40d] G. S. Varner,[42] B. Wang,[30] B. L. Wang,[41] D. Wang,[31] D. Y. Wang,[31] K. Wang,[1,a] L. L. Wang,[1] L. S. Wang,[1] M. Wang,[33] P. Wang,[1] P. L. Wang,[1] S. G. Wang,[31] W. Wang,[1,a] W. P. Wang,[46,a] X. F. Wang,[39] Y. Wang,[37] Y. D. Wang,[14] Y. F. Wang,[1,a] Y. Q. Wang,[22] Z. Wang,[1,a] Z. G. Wang,[1,a] Z. H. Wang,[46,a] Z. Y. Wang,[1] Z. Y. Wang,[1] T. Weber,[22] D. H. Wei,[11] J. B. Wei,[31] P. Weidenkaff,[22] S. P. Wen,[1] U. Wiedner,[4] M. Wolke,[50] L. H. Wu,[1] L. J. Wu,[1] Z. Wu,[1,a] L. Xia,[46,a] L. G. Xia,[39] Y. Xia,[18] D. Xiao,[1] H. Xiao,[47] Z. J. Xiao,[28] Y. G. Xie,[1,a] Q. L. Xiu,[1,a] G. F. Xu,[1] J. J. Xu,[1] L. Xu,[1] Q. J. Xu,[13] Q. N. Xu,[41] X. P. Xu,[37] L. Yan,[49a,49c] W. B. Yan,[46,a] W. C. Yan,[46,a] Y. H. Yan,[18] H. J. Yang,[34] H. X. Yang,[1] L. Yang,[51] Y. X. Yang,[11] M. Ye,[1,a] M. H. Ye,[7] J. H. Yin,[1] B. X. Yu,[1,a] C. X. Yu,[30] J. S. Yu,[26] C. Z. Yuan,[1] W. L. Yuan,[29] Y. Yuan,[1] A. Yuncu,[40b,b] A. A. Zafar,[48] A. Zallo,[20a] Y. Zeng,[18] Z. Zeng,[46,a] B. X. Zhang,[1] B. Y. Zhang,[1,a] C. Zhang,[29] C. C. Zhang,[1] D. H. Zhang,[1] H. H. Zhang,[38] H. Y. Zhang,[1,a] J. Zhang,[1] J. J. Zhang,[1] J. L. Zhang,[1] J. Q. Zhang,[1] J. W. Zhang,[1,a] J. Y. Zhang,[1] J. Z. Zhang,[1] K. Zhang,[1] L. Zhang,[1] S. Q. Zhang,[30] X. Y. Zhang,[33] Y. Zhang,[1] Y. H. Zhang,[1,a] Y. N. Zhang,[41] Y. T. Zhang,[46,a] Yu Zhang,[41] Z. H. Zhang,[6] Z. P. Zhang,[46] Z. Y. Zhang,[51] G. Zhao,[1] J. W. Zhao,[1,a] J. Y. Zhao,[1] J. Z. Zhao,[1,a] Lei Zhao,[46,a] Ling Zhao,[1] M. G. Zhao,[30] Q. Zhao,[1] Q. W. Zhao,[1] S. J. Zhao,[53] T. C. Zhao,[1] Y. B. Zhao,[1,a] Z. G. Zhao,[46,a] A. Zhemchugov,[23,c] B. Zheng,[47] J. P. Zheng,[1,a] W. J. Zheng,[33] Y. H. Zheng,[41] B. Zhong,[28] L. Zhou,[1,a] X. Zhou,[51] X. K. Zhou,[46,a] X. R. Zhou,[46,a] X. Y. Zhou,[1] K. Zhu,[1] K. J. Zhu,[1,a] S. Zhu,[1] S. H. Zhu,[45] X. L. Zhu,[39] Y. C. Zhu,[46,a] Y. S. Zhu,[1] Z. A. Zhu,[1] J. Zhuang,[1,a] L. Zotti,[49a,49c] B. S. Zou,[1] and J. H. Zou[1]

(BESIII Collaboration)

[1]Institute of High Energy Physics, Beijing 100049, People's Republic of China
[2]Beihang University, Beijing 100191, People's Republic of China
[3]Beijing Institute of Petrochemical Technology, Beijing 102617, People's Republic of China
[4]Bochum Ruhr-University, D-44780 Bochum, Germany
[5]Carnegie Mellon University, Pittsburgh, Pennsylvania 15213, USA
[6]Central China Normal University, Wuhan 430079, People's Republic of China
[7]China Center of Advanced Science and Technology, Beijing 100190, People's Republic of China
[8]COMSATS Institute of Information Technology, Lahore, Defence Road, Off Raiwind Road, 54000 Lahore, Pakistan
[9]G.I. Budker Institute of Nuclear Physics SB RAS (BINP), Novosibirsk 630090, Russia
[10]GSI Helmholtzcentre for Heavy Ion Research GmbH, D-64291 Darmstadt, Germany
[11]Guangxi Normal University, Guilin 541004, People's Republic of China
[12]GuangXi University, Nanning 530004, People's Republic of China
[13]Hangzhou Normal University, Hangzhou 310036, People's Republic of China
[14]Helmholtz Institute Mainz, Johann-Joachim-Becher-Weg 45, D-55099 Mainz, Germany
[15]Henan Normal University, Xinxiang 453007, People's Republic of China
[16]Henan University of Science and Technology, Luoyang 471003, People's Republic of China
[17]Huangshan College, Huangshan 245000, People's Republic of China
[18]Hunan University, Changsha 410082, People's Republic of China
[19]Indiana University, Bloomington, Indiana 47405, USA
[20a]INFN Laboratori Nazionali di Frascati, I-00044 Frascati, Italy
[20b]INFN and University of Perugia, I-06100 Perugia, Italy
[21a]INFN Sezione di Ferrara, I-44122 Ferrara, Italy
[21b]University of Ferrara, I-44122 Ferrara, Italy
[22]Johannes Gutenberg University of Mainz, Johann-Joachim-Becher-Weg 45, D-55099 Mainz, Germany
[23]Joint Institute for Nuclear Research, 141980 Dubna, Moscow region, Russia
[24]Justus-Liebig-Universitaet Giessen, II. Physikalisches Institut, Heinrich-Buff-Ring 16, D-35392 Giessen, Germany
[25]KVI-CART, University of Groningen, NL-9747 AA Groningen, The Netherlands
[26]Lanzhou University, Lanzhou 730000, People's Republic of China
[27]Liaoning University, Shenyang 110036, People's Republic of China
[28]Nanjing Normal University, Nanjing 210023, People's Republic of China
[29]Nanjing University, Nanjing 210093, People's Republic of China
[30]Nankai University, Tianjin 300071, People's Republic of China
[31]Peking University, Beijing 100871, People's Republic of China
[32]Seoul National University, Seoul 151-747, Korea
[33]Shandong University, Jinan 250100, People's Republic of China
[34]Shanghai Jiao Tong University, Shanghai 200240, People's Republic of China
[35]Shanxi University, Taiyuan 030006, People's Republic of China
[36]Sichuan University, Chengdu 610064, People's Republic of China
[37]Soochow University, Suzhou 215006, People's Republic of China
[38]Sun Yat-Sen University, Guangzhou 510275, People's Republic of China
[39]Tsinghua University, Beijing 100084, People's Republic of China
[40a]Ankara University, 06100 Tandogan, Ankara, Turkey
[40b]Istanbul Bilgi University, 34060 Eyup, Istanbul, Turkey
[40c]Uludag University, 16059 Bursa, Turkey
[40d]Near East University, Nicosia, North Cyprus, Mersin 10, Turkey
[41]University of Chinese Academy of Sciences, Beijing 100049, People's Republic of China
[42]University of Hawaii, Honolulu, Hawaii 96822, USA
[43]University of Minnesota, Minneapolis, Minnesota 55455, USA
[44]University of Rochester, Rochester, New York 14627, USA
[45]University of Science and Technology Liaoning, Anshan 114051, People's Republic of China
[46]University of Science and Technology of China, Hefei 230026, People's Republic of China
[47]University of South China, Hengyang 421001, People's Republic of China
[48]University of the Punjab, Lahore-54590, Pakistan
[49a]University of Turin, I-10125 Turin, Italy
[49b]University of Eastern Piedmont, I-15121 Alessandria, Italy
[49c]INFN, I-10125 Turin, Italy
[50]Uppsala University, Box 516, SE-75120 Uppsala, Sweden

[51]Wuhan University, Wuhan 430072, People's Republic of China
[52]Zhejiang University, Hangzhou 310027, People's Republic of China
[53]Zhengzhou University, Zhengzhou 450001, People's Republic of China

(Received 1 April 2016; published 21 July 2016)

Using 1.09×10^9 J/ψ events collected by the BESIII experiment in 2012, we study the $J/\psi \to \gamma\eta'\pi^+\pi^-$ process and observe a significant abrupt change in the slope of the $\eta'\pi^+\pi^-$ invariant mass distribution at the proton-antiproton ($p\bar{p}$) mass threshold. We use two models to characterize the $\eta'\pi^+\pi^-$ line shape around 1.85 GeV$/c^2$: one that explicitly incorporates the opening of a decay threshold in the mass spectrum (Flatté formula), and another that is the coherent sum of two resonant amplitudes. Both fits show almost equally good agreement with data, and suggest the existence of either a broad state around 1.85 GeV$/c^2$ with strong couplings to the $p\bar{p}$ final states or a narrow state just below the $p\bar{p}$ mass threshold. Although we cannot distinguish between the fits, either one supports the existence of a $p\bar{p}$ moleculelike state or bound state with greater than 7σ significance.

DOI: 10.1103/PhysRevLett.117.042002

The state $X(1835)$ was first observed by the BESII experiment as a peak in the $\eta'\pi^+\pi^-$ invariant mass distribution in $J/\psi \to \gamma\eta'\pi^+\pi^-$ decays [1]. This observation was later confirmed by BESIII studies of the same process [2] with the mass and width measured to be $M = 1836.5 \pm 3^{+5.6}_{-2.1}$ MeV$/c^2$ and $\Gamma = 190 \pm 9^{+38}_{-36}$ MeV$/c^2$; the $X(1835)$ was also observed in the $\eta K^0_S K^0_S$ channel in $J/\psi \to \gamma\eta K^0_S K^0_S$ decays, where its spin parity was determined to be $J^P = 0^-$ by a partial wave analysis [3]. An anomalously strong enhancement at the proton-antiproton ($p\bar{p}$) mass threshold, dubbed $X(p\bar{p})$, was first observed by BESII in $J/\psi \to \gamma p\bar{p}$ decays [4]; this observation was confirmed by BESIII [5] and CLEO [6]. This enhancement structure was subsequently determined to have spin parity $J^P = 0^-$ by BESIII [7]. Among the various theoretical interpretations on the nature of the $X(1835)$ and $X(p\bar{p})$ [8–12], a particularly intriguing one suggests that the two structures originate from a $p\bar{p}$ bound state [13–17]. If the $X(1835)$ is really a $p\bar{p}$ bound state, it should have a strong coupling to 0^- $p\bar{p}$ systems, in which case the line shape of $X(1835)$ at the $p\bar{p}$ mass threshold would be affected by the opening of the $X(1835) \to p\bar{p}$ decay mode. A study of the $\eta'\pi^+\pi^-$ line shape of $X(1835)$ with high statistical precision therefore provides valuable information that helps clarify the nature of the $X(1835)$ and $X(p\bar{p})$.

In this Letter, we report the observation of a significant abrupt change in slope of the $X(1835) \to \eta'\pi^+\pi^-$ line shape at the $p\bar{p}$ mass threshold in a sample of $J/\psi \to \gamma\eta'\pi^+\pi^-$ events collected in the BESIII detector at the BEPCII e^+e^- storage ring. The η' is reconstructed in its two major decay modes: $\eta' \to \gamma\pi^+\pi^-$ and $\eta' \to \eta\pi^+\pi^-$, $\eta \to \gamma\gamma$. The data sample used in this analysis contains a total of 1.09×10^9 J/ψ decay events [18] accumulated by the BESIII experiment in 2012.

The BESIII detector [19] is a magnetic spectrometer operating at BEPCII [20], a double-ring e^+e^- collider with center of mass energies between 2.0 and 4.6 GeV. The cylindrical core of the BESIII detector consists of a helium-based main drift chamber, a plastic scintillator time-of-flight system, and a CsI(Tl) electromagnetic calorimeter that are all enclosed in a superconducting solenoidal magnet providing a 0.9 T magnetic field. The solenoid is supported by an octagonal flux-return yoke with resistive plate counter muon identifier modules interleaved with steel. The acceptance of charged particles and photons is 93% of the 4π solid angle. The charged-particle momentum resolution at 1 GeV$/c$ is 0.5%; the electromagnetic calorimeter measures 1 GeV photons with an energy resolution of 2.5% (5%) in the barrel (end cap) regions. A GEANT4-based [21] Monte Carlo (MC) simulation software package is used to optimize the event selection criteria, estimate backgrounds, and determine the detection efficiency. The KKMC [22] generator is used to simulate J/ψ production.

The event selection criteria are identical to the previous publication on $J/\psi \to \gamma\eta'\pi^+\pi^-$ at BESIII [2] except for one cut in the $J/\psi \to \gamma\eta'(\to \gamma\pi^+\pi^-)\pi^+\pi^-$ channel: in the previous study, events with $|M_{\gamma\pi^+\pi^-} - m_\eta| < 7$ MeV$/c^2$ are rejected to suppress background from $J/\psi \to \gamma\eta(\to \gamma\pi^+\pi^-)\pi^+\pi^-$; in this analysis, a tighter cut that rejects events with $400\,\text{MeV}/c^2 < M_{\gamma\pi^+\pi^-} < 563\,\text{MeV}/c^2$ is required to suppress background from $J/\psi \to \gamma\eta(\to \pi^0\pi^+\pi^-)\pi^+\pi^-$ as well as background from $J/\psi \to \gamma\eta(\to \gamma\pi^+\pi^-)\pi^+\pi^-$.

The $\eta'\pi^+\pi^-$ invariant mass spectra of the surviving events are shown in Fig. 1, where peaks corresponding to the $X(1835)$, $X(2120)$, $X(2370)$, and η_c [2], and a structure near 2.6 GeV$/c^2$ that has not been seen before are evident for both η' decays. Thanks to the high statistical precision, an abrupt change in slope of the $X(1835)$ line shape at the $p\bar{p}$ mass threshold is evident in both event samples.

An inclusive sample of 10^9 J/ψ decay events that are generated according to the Lund-Charm model [23] and Particle Data Group [24] decay tables is used to study potential background processes. These include events with no real η''s in the final state (non η') and those from $J/\psi \to \pi^0\eta'\pi^+\pi^-$. We use η' mass sideband events to estimate the non-η' background contribution to the

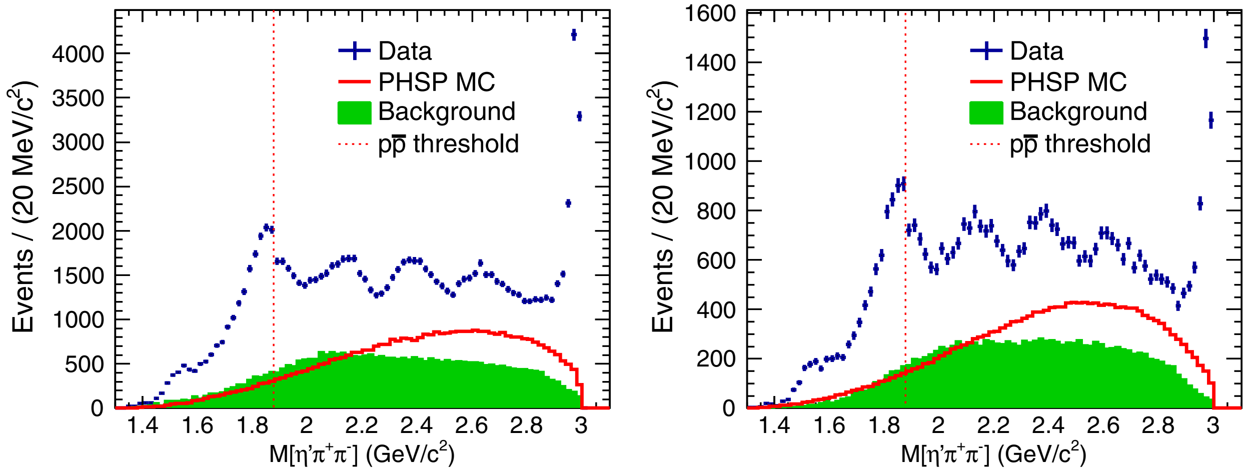

FIG. 1. The $\eta'\pi^+\pi^-$ invariant mass spectra after the application of all selection criteria. The plot on the left side shows the spectrum for events with the $\eta' \to \gamma\pi^+\pi^-$ channel, and that on the right shows the spectrum for the $\eta' \to \eta(\to \gamma\gamma)\pi^+\pi^-$ channel. In both plots, the dots with error bars are data, the shaded histograms are the background, the solid histograms are phase space (PHSP) MC events of $J/\psi \to \gamma\eta'\pi^+\pi^-$ (arbitrary normalization), and the dotted vertical line shows the position of the $p\bar{p}$ mass threshold.

$\eta'\pi^+\pi^-$ invariant mass distribution. For the $J/\psi \to \pi^0\eta'\pi^+\pi^-$ background, we use a one-dimensional data-driven method that first selects $J/\psi \to \pi^0\eta'\pi^+\pi^-$ events from the data to determine the shape of their contribution to the selected $\eta'\pi^+\pi^-$ mass spectrum and reweight this shape by the ratio of MC-determined efficiencies for $J/\psi \to \gamma\eta'\pi^+\pi^-$ and $J/\psi \to \pi^0\eta'\pi^+\pi^-$ events; the total weight after reweighting is the estimated number of $J/\psi \to \pi^0\eta'\pi^+\pi^-$ background events. Our studies of background processes show that neither the four peaks mentioned above nor the abrupt change in the line shape at $2m_p$ is caused by background processes.

We perform simultaneous fits to the $\eta'\pi^+\pi^-$ invariant mass distributions between 1.3 and 2.25 GeV$/c^2$ for both selected event samples with the $f_1(1510)$, $X(1835)$, and $X(2120)$ peaks represented by three efficiency-corrected Breit-Wigner functions convolved with a Gaussian function to account for the mass resolution, where the Breit-Wigner masses and widths are free parameters. The nonresonant $\eta'\pi^+\pi^-$ contribution is obtained from Monte Carlo simulation; the non-η' and $J/\psi \to \pi^0\eta'\pi^+\pi^-$ background contributions are obtained as discussed above. For resonances and the nonresonant $\eta'\pi^+\pi^-$ contribution, the phase space for $J/\psi \to \gamma\eta'\pi^+\pi^-$ is considered: according to the J^P of $f_1(1510)$ and $X(1835)$, $J/\psi \to \gamma f_1(1510)$ and $J/\psi \to \gamma X(1835)$ are S-wave and P-wave processes, respectively; all other processes are assumed to be S-wave processes. Without explicit mention, all components are treated as incoherent contributions. In the simultaneous fits, the masses and widths of resonances, as well as the branching fraction for J/ψ radiative decays to $\eta'\pi^+\pi^-$ final states (including resonances and nonresonant $\eta'\pi^+\pi^-$) are constrained to be the same for both η' decay channels. The fit results are shown in Fig. 2, where it is evident that using a simple Breit-Wigner function to describe the $X(1835)$ line shape fails near the $p\bar{p}$ mass threshold. The $\log\mathcal{L}$ ($\mathcal{L}$ is the combined likelihood of simultaneous fits) of this fit is 630 503.3. Typically, there are two circumstances where an abrupt distortion of a resonance's line shape shows up: a threshold effect caused by the opening of an additional

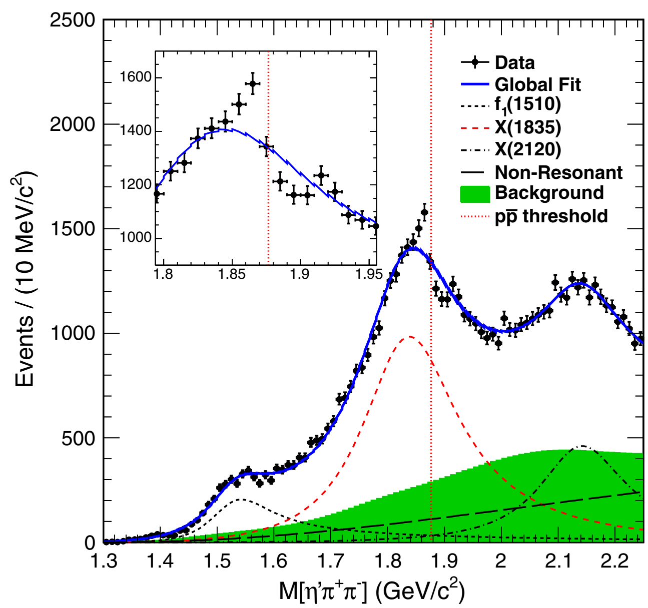

FIG. 2. Fit results with simple Breit-Wigner formulas. The dashed dotted vertical line shows the position of the $p\bar{p}$ mass threshold, the dots with error bars are data, the solid curves are total fit results, the dashed curves are the $X(1835)$, the short-dashed curves are the $f_1(1510)$, the dash-dot curves are the $X(2120)$, and the long-dashed curves are the nonresonant $\eta'\pi^+\pi^-$ fit results; the shaded histograms are background events. The inset shows the data and the global fit between 1.8 and 1.95 GeV$/c^2$.

decay mode, or interference between two resonances. We tried to fit the data for both of these possibilities.

In the first model, we assume the state around $1.85\ \mathrm{GeV}/c^2$ couples to the $p\bar{p}$. The line shape of $\eta'\pi^+\pi^-$ above the $p\bar{p}$ threshold is therefore affected by the opening of the $X(1835)\to p\bar{p}$ decay channel, similar to the distortion of the $f_0(980)\to\pi^+\pi^-$ line shape at the $K\bar{K}$ threshold. To study this, the Flatté formula [25] is used for the $X(1835)$ line shape:

$$T=\frac{\sqrt{\rho_{\mathrm{out}}}}{\mathcal{M}^2-s-i\sum_k g_k^2\rho_k}. \quad (1)$$

Here, T is the decay amplitude, ρ_{out} is the phase space for $J/\psi\to\gamma\eta'\pi^+\pi^-$, $\mathcal{M}$ is a parameter with the dimension of mass, s is the square of the $\eta'\pi^+\pi^-$ system's mass, ρ_k is the phase space for decay mode k, and g_k^2 is the corresponding coupling strength. The term $\sum_k g_k^2\rho_k$ describes how the decay width varies with s. Approximately,

$$\sum_k g_k^2\rho_k\approx g_0^2\left(\rho_0+\frac{g_{p\bar{p}}^2}{g_0^2}\rho_{p\bar{p}}\right), \quad (2)$$

where g_0^2 is the sum of g^2 of all decay modes other than the $X(1835)\to p\bar{p}$, ρ_0 is the maximum two-body decay phase space volume [24], and $g_{p\bar{p}}^2/g_0^2$ is the ratio between the coupling strength to the $p\bar{p}$ channel and the sum of all other channels.

The fit results for this model are shown in Fig. 3. The Flatté model fit has a $\log\mathcal{L}=630549.5$ that is improved over the simple Breit-Wigner one by 46, so the significance of $g_{p\bar{p}}^2/g_0^2$ being nonzero is 9.6σ. In the fit, an additional Breit-Wigner resonance [denoted as "$X(1920)$" in Fig. 3] is needed with a mass of $1918.6\pm3.0\ \mathrm{MeV}/c^2$ and a width of $50.6\pm20.9\ \mathrm{MeV}/c^2$; the statistical significance of this peak is 5.7σ. In the simple Breit-Wigner fit, the significance of $X(1920)$ is negligible. The fit yields $\mathcal{M}=1638.0\pm121.9\ \mathrm{MeV}/c^2$, $g_0^2=93.7\pm35.4(\mathrm{GeV}/c^2)^2$, $g_{p\bar{p}}^2/g_0^2=2.31\pm0.37$, and a product branching fraction of $\mathcal{B}(J/\psi\to\gamma X)\mathcal{B}(X\to\eta'\pi^+\pi^-)=(3.93\pm0.38)\times10^{-4}$. The value of $g_{p\bar{p}}^2/g_0^2$ implies that the couplings between the state around $1.85\ \mathrm{GeV}/c^2$ and the $p\bar{p}$ final states is very large. Following the definitions given in Ref. [26], the pole position is determined by requiring the denominator in Eq. (1) to be zero. The pole nearest to the $p\bar{p}$ mass threshold is found to be $M_{\mathrm{pole}}=1909.5\pm15.9\ \mathrm{MeV}/c^2$ and $\Gamma_{\mathrm{pole}}=273.5\pm21.4\ \mathrm{MeV}/c^2$. Taking the systematic uncertainties (see below) into account, the significance of $g_{p\bar{p}}^2/g_0^2$ being nonzero is larger than 7σ.

In the second model, we assume the existence of a narrow resonance near the $p\bar{p}$ threshold and that the interference between this resonance and the $X(1835)$ produces the line shape distortion. Here, we denote this narrow resonance as "$X(1870)$." For this case we represent the line shape in the vicinity of $1835\ \mathrm{MeV}/c^2$ by the square of T, where

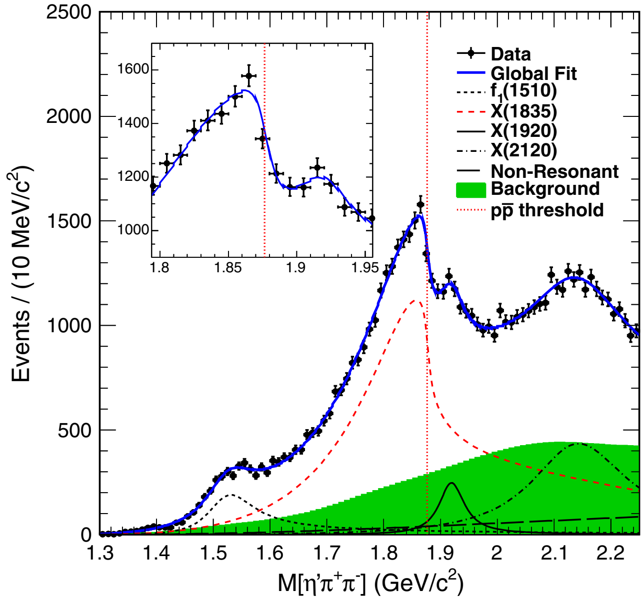

FIG. 3. Fit results of using the Flatté formula. The dashed dotted vertical line shows the position of the $p\bar{p}$ mass threshold, the dots with error bars are data, the solid curves are total fit results, the dashed curves are the state around $1.85\ \mathrm{GeV}/c^2$, the short-dashed curves are the $f_1(1510)$, the dash-dotted curves are the $X(2120)$, the dash-dot-dot-dotted curves are the $X(1920)$, and the long-dashed curves are nonresonant $\eta'\pi^+\pi^-$ fit results; the shaded histograms are background events. The inset shows the data and the global fit between 1.8 and $1.95\ \mathrm{GeV}/c^2$.

$$T=\left(\frac{\sqrt{\rho_{\mathrm{out}}}}{M_1^2-s-iM_1\Gamma_1}+\frac{\beta e^{i\theta}\sqrt{\rho_{\mathrm{out}}}}{M_2^2-s-iM_2\Gamma_2}\right). \quad (3)$$

Here, ρ_{out} and s have the same meaning as they had in Eq. (1); M_1, Γ_1, M_2, and Γ_2 represent the masses and widths of the $X(1835)$ and $X(1870)$ resonances, respectively; and β and θ are the relative $\eta'\pi^+\pi^-$ coupling strengths and the phase between the two resonances.

The fit results for the second model are shown in Fig. 4. The $\log\mathcal{L}$ of this fit is 630 540.3, which is improved by 37 with four additional parameters over that for the fit using one simple Breit-Wigner function. The $X(1835)$ mass is $1825.3\pm2.4\ \mathrm{MeV}/c^2$ and the width is $245.2\pm13.1\ \mathrm{MeV}/c^2$; the $X(1870)$ mass is $1870.2\pm2.2\ \mathrm{MeV}/c^2$ and the width is $13.0\pm6.1\ \mathrm{MeV}/c^2$, with a statistical significance that is 7.9σ. It is known that there are two nontrivial solutions in a fit using a coherent sum of two Breit-Wigner functions [27]. In the parametrization of Eq. (3), the two solutions share the same M_1, Γ_1, M_2, and Γ_2, but have different values of β and θ, which means that the only observable difference between the solutions are branching fractions of the two Breit-Wigner functions. The product branching fractions with constructive interference are $\mathcal{B}[J/\psi\to\gamma X(1835)]\mathcal{B}[X(1835)\to\eta'\pi^+\pi^-]=(3.01\pm0.17)\times10^{-4}$ and $\mathcal{B}[J/\psi\to\gamma X(1870)]\mathcal{B}[X(1870)\to\eta'\pi^+\pi^-]=(2.03\pm0.12)\times10^{-7}$, while the solution with destructive interference

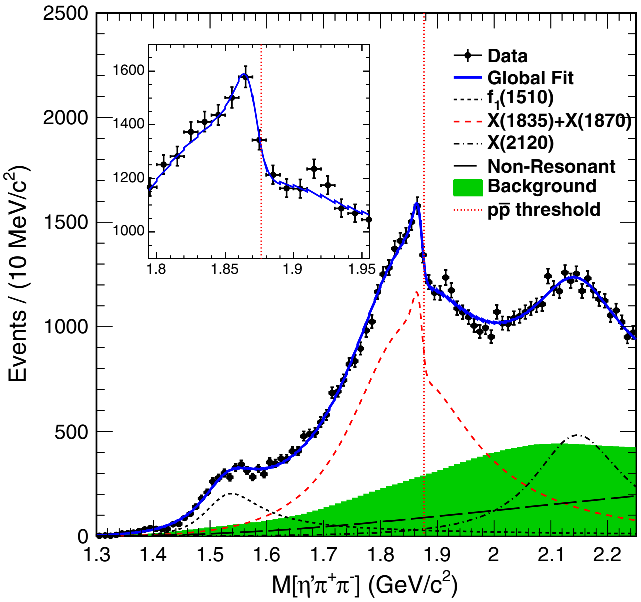

FIG. 4. Fit results of using a coherent sum of two Breit-Wigner amplitudes. The dashed dotted vertical line shows the position of the $p\bar{p}$ mass threshold, the dots with error bars are data, the solid curves are total fit results, the dashed curves are the sum of $X(1835)$ and $X(1870)$, the short-dashed curves are the $f_1(1510)$, the dash-dotted curves are the $X(2120)$, the long-dashed curves are nonresonant $\eta'\pi^+\pi^-$ fit results, and the shaded histograms are background events. The inset shows the data and the global fit between 1.8 and 1.95 GeV$/c^2$.

gives $\mathcal{B}[J/\psi\to\gamma X(1835)]\mathcal{B}[X(1835)\to\eta'\pi^+\pi^-]=(3.72\pm 0.21)\times 10^{-4}$, and $\mathcal{B}[J/\psi\to\gamma X(1870)]\mathcal{B}[X(1870)\to \eta'\pi^+\pi^-]=(1.57\pm 0.09)\times 10^{-5}$. In this model, the $X(1920)$ is not included in the fit because its significance is just 3.9σ. Considering systematic uncertainties (see below), the significance of $X(1870)$ is larger than 7σ.

The systematic uncertainties come from data-MC differences in the tracking, photon detection and particle identification efficiencies, the kinematic fit, requirements on the invariant mass distribution of $\gamma\gamma$, signal selection of ρ^0, η, and η', total number of J/ψ events, branching fractions for intermediate states decays, fit ranges, background descriptions, mass resolutions, and the intermediate structure of $\pi^+\pi^-$. In the first model, the dominant terms are the fit range, the background description, and the intermediate structure of $\pi^+\pi^-$. Considering all systematic uncertainties, the final result is shown in Table I. For the second model, the dominant two systematic sources are the background description and the intermediate structure of $\pi^+\pi^-$. Considering all systematic uncertainties, the final result is shown in Table II.

In summary, the $J/\psi\to\gamma\eta'\pi^+\pi^-$ process is studied with 1.09×10^9 J/ψ events collected at the BESIII experiment in 2012. We observed a significant distortion of the $\eta'\pi^+\pi^-$ line shape near the $p\bar{p}$ mass threshold that cannot be accommodated by an ordinary Breit-Wigner resonance function. Two typical models for such a line shape are used to fit the data. The first model assumes the state around 1.85 GeV$/c^2$ couples with the $p\bar{p}$ and the distortion reflects the opening of the $p\bar{p}$ decay channel. The fit result for this model yields a strong coupling between the broad structure and the $p\bar{p}$ of $g^2_{p\bar{p}}/g^2_0 = 2.31\pm 0.37^{+0.83}_{-0.60}$, with a statistical significance larger than 7σ for being nonzero. The pole nearest to the $p\bar{p}$ mass threshold of this state is located at $M_{\rm pole} = 1909.5\pm 15.9({\rm stat})^{+9.4}_{-27.5}({\rm syst})$ MeV$/c^2$ and $\Gamma_{\rm pole} = 273.5\pm 21.4({\rm stat})^{+6.1}_{-64.0}({\rm syst})$ MeV$/c^2$. The second model assumes the distortion reflects interference between the $X(1835)$ and another resonance with mass close to the $p\bar{p}$ mass threshold. A fit with this model uses a coherent sum of two interfering Breit-Wigner amplitudes to describe the $\eta'\pi^+\pi^-$ mass spectrum around 1.85 GeV$/c^2$. This fit yields a narrow resonance below the $p\bar{p}$ mass threshold with $M=1870.2\pm 2.2({\rm stat})^{+2.3}_{-0.7}({\rm syst})$ MeV$/c^2$ and $\Gamma = 13.0\pm 6.1({\rm stat})^{+2.1}_{-3.8}({\rm syst})$ MeV$/c^2$, with a statistical significance larger than 7σ. With current data, both models fit the data well with fit qualities, and both suggest the existence of a state, either a broad state with strong couplings to the $p\bar{p}$, or a narrow state just below the $p\bar{p}$ mass threshold. For the broad state above the $p\bar{p}$ mass threshold, its strong

TABLE I. Fit results of using the Flatté formula. The first errors are statistical errors, and the second errors are systematic errors; the branching ratio is the product of $\mathcal{B}(J/\psi\to\gamma X)$ and $\mathcal{B}(X\to\eta'\pi^+\pi^-)$.

The state around 1.85 GeV$/c^2$	
$\mathcal{M}$ (MeV$/c^2$)	$1638.0\pm 121.9^{+127.8}_{-254.3}$
g_0^2 [(GeV$/c^2)^2$]	$93.7\pm 35.4^{+47.6}_{-43.9}$
$g^2_{p\bar{p}}/g^2_0$	$2.31\pm 0.37^{+0.83}_{-0.60}$
$M_{\rm pole}$ (MeV$/c^2$)	$1909.5\pm 15.9^{+9.4}_{-27.5}$
$\Gamma_{\rm pole}$ (MeV$/c^2$)	$273.5\pm 21.4^{+6.1}_{-64.0}$
Branching ratio	$(3.93\pm 0.38^{+0.31}_{-0.84})\times 10^{-4}$

TABLE II. Fit results using a coherent sum of two Breit-Wigner amplitudes. The first errors are statistical errors, and the second errors are systematic errors; the branching ratio (B.R.) is the product of $\mathcal{B}(J/\psi\to\gamma X)$ and $\mathcal{B}(X\to\eta'\pi^+\pi^-)$.

$X(1835)$	
Mass (MeV$/c^2$)	$1825.3\pm 2.4^{+17.3}_{-2.4}$
Width (MeV$/c^2$)	$245.2\pm 13.1^{+4.6}_{-9.6}$
B.R. (constructive interference)	$(3.01\pm 0.17^{+0.26}_{-0.28})\times 10^{-4}$
B.R. (destructive interference)	$(3.72\pm 0.21^{+0.18}_{-0.35})\times 10^{-4}$
$X(1870)$	
Mass (MeV$/c^2$)	$1870.2\pm 2.2^{+2.3}_{-0.7}$
Width (MeV$/c^2$)	$13.0\pm 6.1^{+2.1}_{-3.8}$
B.R. (constructive interference)	$(2.03\pm 0.12^{+0.43}_{-0.70})\times 10^{-7}$
B.R. (destructive interference)	$(1.57\pm 0.09^{+0.49}_{-0.86})\times 10^{-5}$

couplings to the $p\bar{p}$ suggest the existence of a $p\bar{p}$ moleculelike state. For the narrow state just below the $p\bar{p}$ mass threshold, its very narrow width suggests that it is an unconventional meson, most likely a $p\bar{p}$ bound state. So both fits support the existence of a $p\bar{p}$ moleculelike or bound state. With current statistics, more sophisticated models such as a mixture of above two models cannot be ruled out. In order to elucidate further the nature of the states around 1.85 GeV/c^2, more data are needed to further study the $J/\psi \to \gamma\eta'\pi^+\pi^-$ process. Also, line shapes for other decay modes should be studied near the $p\bar{p}$ mass threshold, including further studies of $J/\psi \to \gamma p\bar{p}$ and $J/\psi \to \gamma\eta K_S^0 K_S^0$.

BESIII Collaboration thanks the staff of BEPCII and the IHEP computing center for their strong support. This work is supported in part by the National Key Basic Research Program of China under Contract No. 2015CB856700; the National Natural Science Foundation of China (NSFC) under Contracts No. 11235011, No. 11322544, No. 11335008, and No. 11425524; the Chinese Academy of Sciences (CAS) Large-Scale Scientific Facility Program; the CAS Center for Excellence in Particle Physics (CCEPP); the Collaborative Innovation Center for Particles and Interactions (CICPI); the Joint Large-Scale Scientific Facility Funds of the NSFC and CAS under Contracts No. U1232201 and No. U1332201; the CAS under Contracts No. KJCX2-YW-N29 and No. KJCX2-YW-N45; the 100 Talents Program of the CAS; the National 1000 Talents Program of China; INPAC and Shanghai Key Laboratory for Particle Physics and Cosmology; Istituto Nazionale di Fisica Nucleare, Italy; the Joint Large-Scale Scientific Facility Funds of the NSFC and the CAS under Contract No. U1532257; the Joint Large-Scale Scientific Facility Funds of the NSFC and the CAS under Contract No. U1532258; Koninklijke Nederlandse Akademie van Wetenschappen (KNAW) under Contract No. 530-4CDP03; the Ministry of Development of Turkey under Contract No. DPT2006K-120470; the Swedish Research Council; the U.S. Department of Energy under Contracts No. DE-FG02-05ER41374, No. DE-SC-0010504, and No. DE-SC0012069; the U.S. National Science Foundation; the University of Groningen (RuG) and the Helmholtzzentrum fuer Schwerionenforschung GmbH (GSI), Darmstadt; the WCU Program of the National Research Foundation of Korea under Contract No. R32-2008-000-10155-0.

[a]Also at State Key Laboratory of Particle Detection and Electronics, Beijing 100049, Hefei 230026, People's Republic of China.
[b]Also at Bogazici University, 34342 Istanbul, Turkey.
[c]Also at the Moscow Institute of Physics and Technology, Moscow 141700, Russia.
[d]Also at the Functional Electronics Laboratory, Tomsk State University, Tomsk, 634050, Russia.
[e]Also at the Novosibirsk State University, Novosibirsk, 630090, Russia.
[f]Also at the NRC "Kurchatov Institute", PNPI, 188300, Gatchina, Russia.
[g]Also at University of Texas at Dallas, Richardson, Texas 75083, USA.
[h]Also at Istanbul Arel University, 34295 Istanbul, Turkey.
[i]Present address: Currently at DESY, 22607 Hamburg, Germany.

[1] M. Ablikim *et al.* (BES Collaboration), Phys. Rev. Lett. **95**, 262001 (2005).
[2] M. Ablikim *et al.* (BESIII Collaboration), Phys. Rev. Lett. **106**, 072002 (2011).
[3] M. Ablikim *et al.* (BESIII Collaboration), Phys. Rev. Lett. **115**, 091803 (2015).
[4] J. Z. Bai *et al.* (BES Collaboration), Phys. Rev. Lett. **91**, 022001 (2003).
[5] M. Ablikim *et al.* (BESIII Collaboration), Chin. Phys. C **34**, 421 (2010).
[6] J. P. Alexander *et al.* (CLEO Collaboration), Phys. Rev. D **82**, 092002 (2010).
[7] M. Ablikim *et al.* (BESIII Collaboration), Phys. Rev. Lett. **108**, 112003 (2012).
[8] T. Huang and S. L. Zhu, Phys. Rev. D **73**, 014023 (2006).
[9] N. Kochelev and D. P. Min, Phys. Lett. B **633**, 283 (2006).
[10] G. Hao, C. F. Qiao, and A. Zhang, Phys. Lett. B **642**, 53 (2006).
[11] B. A. Li, Phys. Rev. D **74**, 034019 (2006).
[12] X. H. Liu, Y. J. Zhang, and Q. Zhao, Phys. Rev. D **80**, 034032 (2009).
[13] S. L. Zhu and C. S. Gao, Commun. Theor. Phys. **46**, 291 (2006).
[14] J. P. Dedonder, B. Loiseau, B. El-Bennich, and S. Wycech, Phys. Rev. C **80**, 045207 (2009).
[15] G. J. Ding, R. G. Ping, and M. L. Yan, Eur. Phys. J. A **28**, 351 (2006).
[16] C. Liu, Eur. Phys. J. C **53**, 413 (2008).
[17] Z. G. Wang and S. L. Wan, J. Phys. G **34**, 505 (2007).
[18] M. Ablikim *et al.* (BESIII Collaboration), Chin. Phys. C **36**, 915 (2012).
[19] M. Ablikim *et al.* (BESIII Collaboration), Nucl. Instrum. Methods Phys. Res., Sect. A **614**, 345 (2010).
[20] J. Z. Bai *et al.* (BES Collaboration), Nucl. Instrum. Methods Phys. Res., Sect. A **344**, 319 (1994); **458**, 627 (2001).
[21] S. Agostinelli *et al.* (GEANT4 Collaboration), Nucl. Instrum. Methods Phys. Res., Sect. A **506**, 250 (2003).
[22] S. Jadach, B. F. L. Ward, and Z. Was, Comput. Phys. Commun. **130**, 260 (2000); Phys. Rev. D **63**, 113009 (2001).
[23] J. C. Chen, G. S. Huang, X. R. Qi, D. H. Zhang, and Y. S. Zhu, Phys. Rev. D **62**, 034003 (2000).
[24] K. A. Olive *et al.* (Particle Data Group), Chin. Phys. C **38**, 090001 (2014).
[25] S. M. Flatté, Phys. Lett. B **63**, 224 (1976).
[26] B. S. Zou and D. V. Bugg, Phys. Rev. D **48**, R3948 (1993).
[27] K. Zhu, X. H. Mo, C. Z. Yuan, and P. Wang, Int. J. Mod. Phys. A **26**, 4511 (2011).